

## Simultaneous Measurement of Diffusion along Multiple Directions

Xiao-Ping Tang,<sup>†</sup> Eric E. Sigmund,<sup>‡</sup> and Yi-Qiao Song<sup>\*‡</sup>

Department of Physics, University of Nevada, Reno, Nevada 89557, and Schlumberger-Doll Research, Old Quarry Road, Ridgefield, Connecticut 06877

Received August 31, 2004; E-mail: ysong@slb.com

In anisotropic materials, such as liquid crystals<sup>1</sup> and stretched polymer electrolytes,<sup>2</sup> diffusion can be highly anisotropic, and the anisotropy may differ among structural phases and vary with the electrochemical force. At the microscale, diffusion in porous media may inevitably exhibit anisotropy due to the restriction and pore connectivity.<sup>3</sup> Biological tissues, such as skeletal muscles,<sup>4</sup> restrict diffusion in some structural orientations. Diffusion anisotropy is measured by comparing the diffusion coefficient along several noncollinear directions.<sup>5</sup> However, the existing methods generally require many acquisitions,<sup>5–7</sup> and the resulting long experimental time may limit their application in metastable systems and in vivo/in situ studies. The present work demonstrates a fast NMR technique to measure diffusion along multiple noncollinear directions simultaneously and thus obtain the full diffusion tensor in one scan.

The diffusion effects on spin echoes in a magnetic field gradient was first described by Hahn.<sup>8</sup> The Larmor precession of the transverse magnetization in the field gradient causes a spatial modulation of the magnetization. Diffusion randomly disrupts the modulation and produces an exponential decay of the echo signal. As more RF pulses are used in a sequence, a more complex magnetization evolution pattern can be created, giving rise to many echoes with different diffusion sensitivities. The behavior of these echoes is described by the coherence pathway (CPW) formalism.<sup>9</sup> A coherence pathway is defined as a specific pattern of the magnetization states,  $Q$ . The role of an RF pulse is to transfer magnetization from one state to another. In general, the echo decay is of the form  $S(Q) = A(Q) \exp(-\sum_{ij} b_{ij} D_{ij})$ , where  $D_{ij}$  is the diffusion tensor element, and the weighting tensor element,  $b_{ij}$ , is determined by  $Q$  and the gradient pattern.<sup>10</sup>  $A(Q)$  depends only on the RF pulses and CPW.

It has been shown<sup>10</sup> recently that 13 echoes, each with a different diffusion weighting, can be produced using the 4-pulse multiple-modulation–multiple-echo (MMME) sequence,  $\alpha_1 - \tau - \alpha_2 - 3\tau - \alpha_3 - 9\tau - \alpha_4 - \text{acquisition}$ , in the presence of a constant field gradient, where  $\alpha_1$ ,  $\alpha_2$ ,  $\alpha_3$ , and  $\alpha_4$  are the RF pulses. The 13 echoes originate from different CPWs and appear separately in the time domain. Since the  $b$  values of the echoes are different, one MMME scan is adequate to determine the diffusion constant along the one direction of the field gradient. The total echo amplitude is about 4 times that of the Hahn echo.

Now, we demonstrate a method for measuring diffusion along multiple directions and thus obtaining all diffusion tensor elements simultaneously in one scan. To illustrate the essence of the method, let us first consider a constant  $z$ -gradient during the entire sequence and only one  $x$ -gradient pulse ( $G_{x2}$ ) during the  $9\tau$  period. Since only the latter nine echoes exhibit the transverse magnetization during the  $9\tau$  period, they alone are modulated by  $G_{x2}$ . To form the latter nine echoes, another identical  $G_{x2}$  gradient pulse must be applied after the fourth echo to unwind the modulation. Thus,

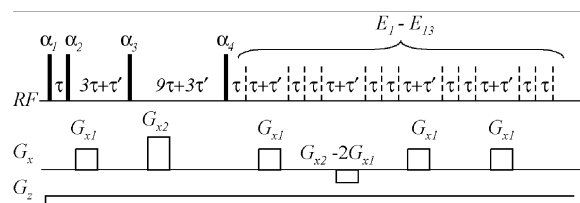


**Figure 1.** The 4-pulse MMME2D sequence. Extra periods  $\tau'$  and  $3\tau'$  are added to the original MMME<sup>10</sup> to facilitate the application of the gradient pulses. The 13 echoes (dashed lines) form five groups; the first group consists of the first echo and the next four groups three echoes each. After the first, fourth, seventh, and 10th echoes, an  $x$ -gradient pulse is applied. The duration of all  $x$ -gradient pulses is  $\delta$ .

diffusion along  $x$  can induce decay only for the latter nine echoes. On the other hand, all echoes experience different amounts of decay due to diffusion along  $z$ . As a result, one scan produces 13 echoes with a different range of decay along  $x$  and  $z$  and thus allows the measurement of the two-dimensional diffusion tensor. We label this type of sequence MMME2D (2D refers to the dimensions of the gradient directions).

A generalized sequence (Figure 1) uses a constant  $z$ -gradient and two  $x$ -gradient pulses,  $G_{x1}$  and  $G_{x2}$ , of  $\delta$  duration, applied after  $\alpha_2$  and  $\alpha_3$ , respectively. Since the  $b_{ij}$  elements, when viewed as a vector, are, in general, not collinear for all echoes, one scan provides 13 independent data to determine the diffusion tensor. In this regard, one MMME2D scan is similar to 13 stimulated echo scans at different gradient directions. The RF pulse factor,  $A(Q)$ , can be determined theoretically<sup>10</sup> or by a reference scan with an identical RF pulse set, but with different  $\tau$ ,  $\tau'$ , and  $x$ -gradients. The amplitude ratio between the corresponding echoes of the two scans, 1 and 2, directly probes diffusion:

$$S^1(Q)/S^2(Q) = \exp\{-\Delta b_{zz} D_{zz} - \Delta b_{xx} D_{xx} - 2\Delta b_{xz} D_{xz}\} \quad (1)$$

where  $\Delta b_{xx}$ ,  $\Delta b_{zz}$ ,  $\Delta b_{xz}$  are the differences of the  $b$  values between the two scans.

Anisotropic diffusion was studied on an asparagus sample of 4 mm diameter cut from the center of a 12 mm diameter stalk. This system is composed of bundles of elongated cells along the stalk axis. The cell membrane is known to reduce water permeation such that diffusion is limited particularly transverse to the stalk axis. As a result, the molecular diffusion has been shown to be anisotropic and smaller than the bulk value on a time scale of 50 ms.<sup>11</sup> Diffusion along six noncollinear directions was measured by the conventional pulsed-field gradient (PFG) method to determine the anisotropic diffusion tensor with diagonal elements  $D_{zz}/D_{xx}/D_{yy} = 1.5/1.1/1.1 \times 10^{-5}$  cm<sup>2</sup>/s and vanishing off-diagonal elements. It shows that the principal axes of the diffusion tensor are parallel to the lab frame axes.

The MMME2D experiment on the asparagus sample is displayed in Figure 2. The amplitude ratio ( $S^1/S^2$ ) of the corresponding echoes

<sup>†</sup> University of Nevada.

<sup>‡</sup> Schlumberger-Doll Research.

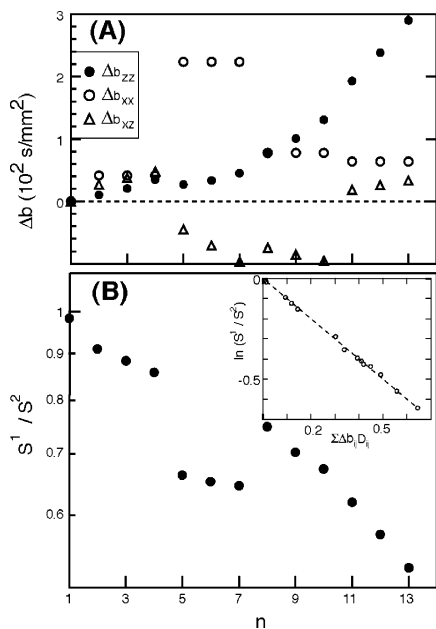


**Figure 2.** Figure 2. MMME2D results on the asparagus sample. (A) Plot of the calculated three  $\Delta b$  elements versus the echo number,  $n$ . (B) Plot of the measured amplitude ratios versus  $n$ . The gradual signal decay is due mostly to longitudinal diffusion ( $D_{zz}$ ), whereas the abrupt drop of echoes 5–7 reflects transverse diffusion ( $D_{xx}$ ). Inset: plot of the amplitude ratios versus the full diffusion weighting argument demonstrating the quality of the fit. Both scans used  $\alpha_1/\alpha_2/\alpha_3/\alpha_4 = 55/71/71/110^\circ$  to reduce the amplitude variation among the 13 echoes (ref 10). The two scans use (1)  $G_z/G_{x1}/G_{x2} = 2.5/15/-15$  G/cm,  $\tau/\tau'/\delta = 1.5/1.5/1.0$  ms; and (2)  $G_z/G_{x1}/G_{x2} = 2.5/0/0$  G/cm,  $\tau/\tau'/\delta = 1.0/1.5/1.0$  ms.

was used to scale out the  $A(Q)$  factors. It thus measures solely the diffusion effect. We used the contrasting patterns of diffusion weighting ( $\Delta b$ ) versus the echo number ( $n$ ) for different elements, which is desirable for reducing correlated errors between the diffusion tensor elements. The echo amplitude ratios in Figure 2B show a gradual reduction due to diffusion along  $z$  and two steps between echoes 4 and 5 and between echoes 7 and 8 due to diffusion along  $x$ , qualitatively correlated to the  $\Delta b$  patterns in Figure 2A. A least-squares fit of the echo amplitude ratios by Equation 1 obtains  $D_{zz}/D_{xx}/D_{zx} = 1.5/1.2/0.01 \times 10^{-5}$  cm<sup>2</sup>/s, with the overall error estimated at about  $10^{-6}$  cm<sup>2</sup>/s. Thus, the anisotropy is correctly reproduced by the MMME2D experiment. Similar experiments were conducted on a bulk water sample finding  $D_{zz}/D_{xx}/D_{zx} = 1.8/1.7/0.1 \times 10^{-5}$  cm<sup>2</sup>/s, consistent with the expected diffusion isotropy.

In summary, this work demonstrates for the first time a one-scan NMR method for concurrent measurement of anisotropic

diffusion tensors. The 4-pulse sequence illustrated here is an example of the broad MMME class of sequences.<sup>10</sup> The 5-pulse MMME, producing 40 echoes, may bring further improvement and allow a one-scan measurement of a 3D diffusion tensor. It is possible to extend the MMME technique to acquire chemical shift resolution (perhaps with limited resolution), thus enabling a one-scan DOSY.<sup>12</sup> MMME2D can provide a new tool for in situ study of anisotropy in chemical systems. For example, many solid electrolytes<sup>13</sup> and polyelectrolytes<sup>14</sup> display anisotropy that reflects either structural (e.g., stacked aluminosilicate layers) or chemical (e.g., water content, pH) properties. The progress of chemical reactions and material degradation might be monitored through the anisotropy. Many nanoscale structures can be viewed as quasi-1D<sup>15</sup> or 2D<sup>16</sup> pores. Owing to the geometric confinement and the interactions with pore walls, the chemical bonding of gases and liquids, such as water,<sup>15,16</sup> within the nanopores can vary from the bulk phases. For example, diffusion anisotropy might be used to distinguish molecules inside or outside the nanotubes, providing a viable means for monitoring the uptake of gases and liquids into the nanotubes. MMME can be used in stray field NMR, and the limitation due to short  $T_2$  is similar to that of the conventional method.<sup>8</sup>

**Acknowledgment.** We thank D. Raftery for comments.

## References

- (1) de Gennes, P. G. *The Physics of Liquid Crystals*; Oxford University Press: Oxford, 1974.
- (2) Golodnitsky, D.; Livshits, E.; Ulus, A.; Barkay, Z.; Lapidis, I.; Peled, E.; Chung, S. H.; Greenbaum, S. *J. Phys. Chem. A* **2001**, *105*, 10098–10106.
- (3) Stallmach, F.; Kärger, J.; Krause, C.; Jeschke, M.; Oberhagemann, U. *J. Am. Chem. Soc.* **2000**, *122*, 9237–9242.
- (4) Napadow, V. J.; Chen, Q.; Mai, V.; So, P. T. C.; Gilbert, R. J. *Biophys. J.* **2001**, *80*, 2968–2975.
- (5) Callaghan, P. T. *Principles of Nuclear Magnetic Resonance Microscopy*; Oxford University Press: Oxford, 1993.
- (6) Furó, I.; Dvinskikh, S. *Magn. Reson. Chem.* **2002**, *40*, S3–S14.
- (7) Basser, P. J.; Mattiello, J.; LeBihan, D. *Biophys. J.* **1994**, *66*, 259–267.
- (8) Hahn, E. L. *Phys. Rev.* **1950**, *80*, 580–594.
- (9) Kaiser, R.; Bartholdi, E.; Ernst, R. R. *J. Chem. Phys.* **1974**, *60*, 2966–2979.
- (10) Song, Y.-Q.; Tang, X.-P. *J. Magn. Reson.* **2004**, *170*, 136–148.
- (11) Boujraf, S.; Luypaert, R.; Eisendrath, H.; Osteaux, M. *Magn. Reson. Mater. Phys. Bio. Med.* **2001**, *13*, 82–90.
- (12) Morris, K. F.; Johnson, C. S., Jr. *J. Am. Chem. Soc.* **1992**, *114*, 3139–3141.
- (13) Hutchison, J. C.; Bissessur, R.; Shriver, D. F. *Chem. Mater.* **1996**, *8*, 1597–1599.
- (14) Chen, C.-H.; Postlethwaite, T. A.; Hutchison, J. E.; Samulski, E. T.; Murray, R. W. *J. Phys. Chem.* **1995**, *99*, 8804–8811.
- (15) Mashl, R. J.; Joseph, S.; Aluru, N. R.; Jakobsson E. *Nano Lett.* **2003**, *3*, 589–592.
- (16) Raviv, U.; Laurat, P.; Klein, J. *Nature* **2001**, *413*, 51–54.

JA0447457